Figure S1

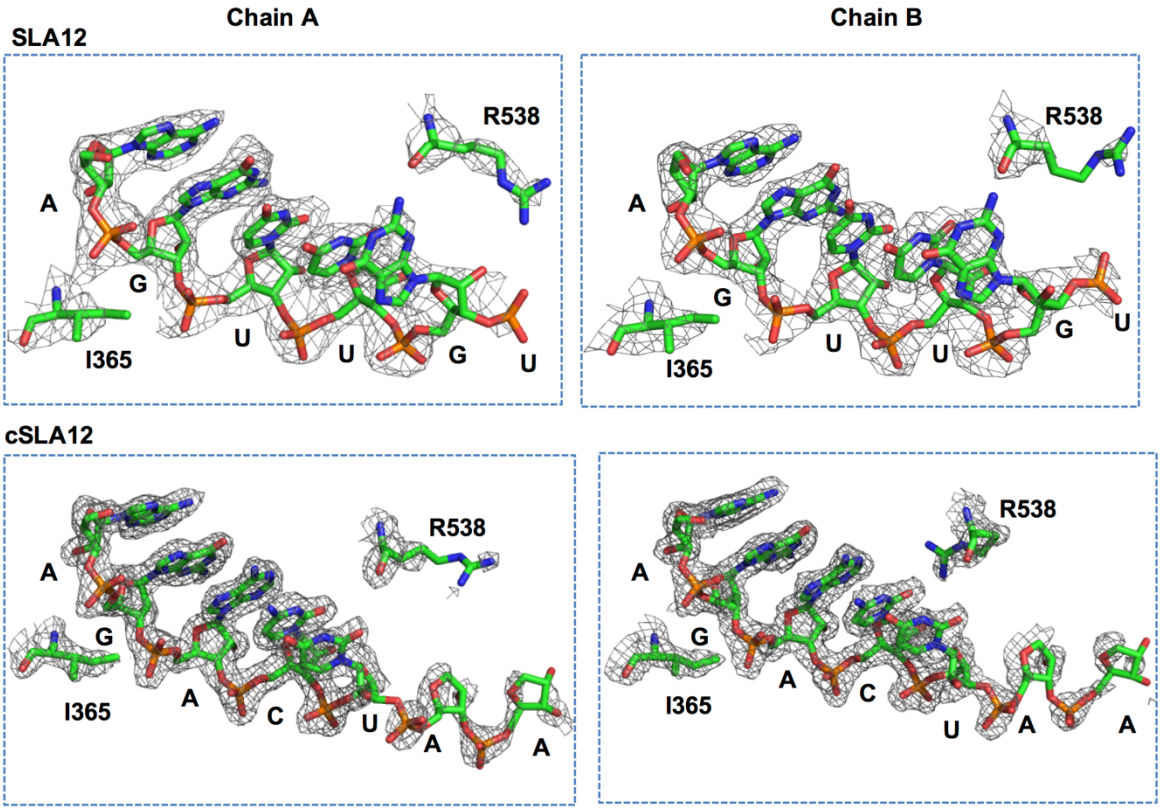

Supplemental Fig S1. Electron density of R538 RNA binding. RNA, R538 and I365 (labelled) residues shown as sticks with electron density represented by grey mesh generated from 2Fo-Fc map and contoured to 1.0 $\boldsymbol{\sigma}$. The two chains from each SLA12 and cSLA12 (PDB accession code: 2JLU (11)) are shown highlighting complete density for R538 in chain A of SLA12 and chain B of cSLA12.

Figure S2

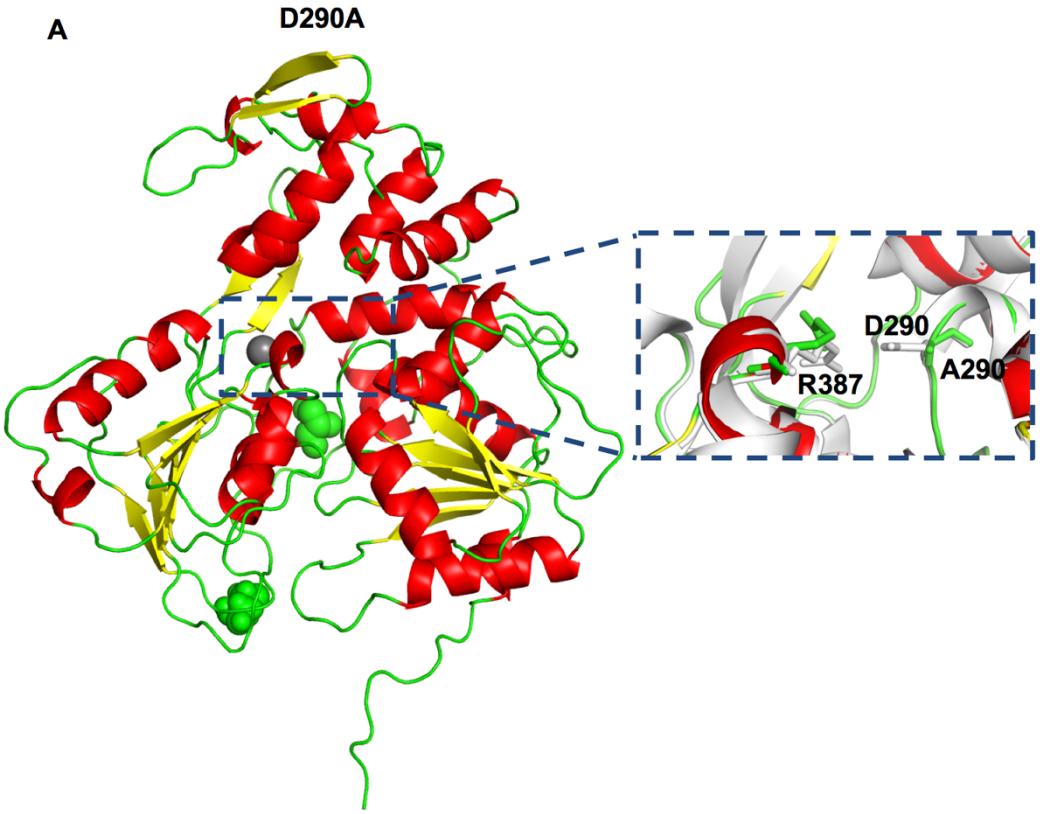

Supplemental Fig S2. NS3H D290A structure. (A) NS3H D290A shown in cartoon representation with secondary structure colouring; α-helices shown in red, β-strands in yellow, loop regions in green, bound chloride ion shown in grey and glycerol molecules in green. Inset, free NS3H (PDB accession code: 2JLQ (11)) D290 R387 charge interaction is shown in grey superimposed with the D290A structure.

Figure S3

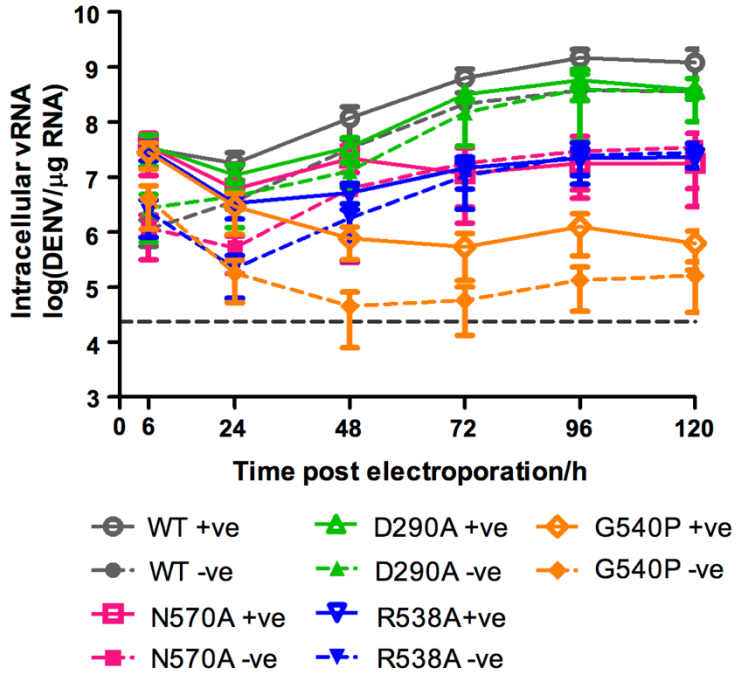

Supplemental Fig S3. Kinetics of positive and negative vRNA synthesis for wild-type and the NS3 mutants. Total RNA extracted from BHK-21 transfected cells and subjected to positive and negative strand synthesis by real-time RT-PCR. The grey dotted line represents the detection level of uninfected control.

Figure S4

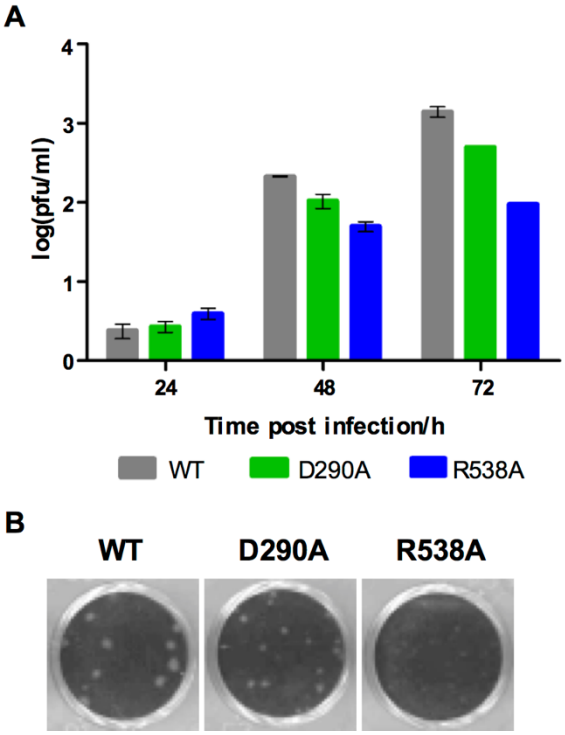

Supplemental Fig S4. Infectivity of the NS3 mutant viruses in C6/36. Supernatants from BHK-21 transfected cells were used to infect C6/36 and (A) infectious virus production is assayed by plaque assay. (B) Plaque morphologies of the NS3 mutant viruses obtained from C6/36 expansion.

Figure S5

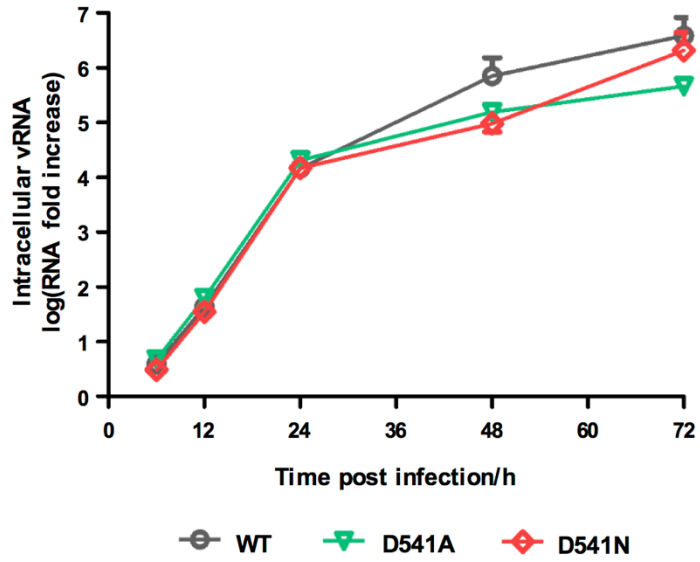

Supplemental Fig S5. Intracellular Growth Kinetics of NS3 Mutant Viruses D541A and D541N. Virus generated from C6/36 transfection used to infect BHK21 cells at MOI 0.3 and replication kinetics followed over 3 days measuring the vRNA using NS1 primers (results reported as RNA fold increase with respect to uninfected control).